International Journal of Mass Spectrometry xxx (2013) xxx–xxx

Contents lists available at SciVerse ScienceDirect

International Journal of Mass Spectrometry

journal homepage: www.elsevier.com/locate/ijms

# ISOLTRAP's multi-reflection time-of-flight mass separator/spectrometer

R.N. Wolf[a,*], F. Wienholtz[a], D. Atanasov[b], D. Beck[b], K. Blaum[c], Ch. Borgmann[c], F. Herfurth[b], M. Kowalska[d], S. Kreim[c,d], Yu. A. Litvinov[b,c], D. Lunney[e], V. Manea[e], D. Neidherr[b], M. Rosenbusch[a], L. Schweikhard[a], J. Stanja[f], K. Zuber[f]

[a] Institut für Physik, Ernst-Moritz-Arndt Universität Greifswald, Felix-Hausdorff-Str. 6, 17487 Greifswald, Germany
[b] GSI Helmholtzzentrum für Schwerionenforschung GmbH, Planckstraße 1, 64291 Darmstadt, Germany
[c] Max-Planck-Institut für Kernphysik, Saupfercheckweg 1, 69117 Heidelberg, Germany
[d] CERN, 1211 Geneva 23, Switzerland
[e] CSNSM-IN2P3-CNRS, Université Paris-Sud, 91405 Orsay, France
[f] Institut für Kern- und Teilchenphysik, Technische Universität Dresden, 01069 Dresden, Germany

ARTICLE INFO

*Article history:*
Received 16 February 2013
Received in revised form 26 March 2013
Accepted 29 March 2013
Available online xxx

*Keywords:*
MR-ToF mass separator
Isobar purification
Radioactive ion beam
ISOLTRAP
Penning trap mass spectrometer
Mass of $^{137}$Eu nuclide

ABSTRACT

The online precision mass spectrometer ISOLTRAP at ISOLDE/CERN was recently upgraded by adding a multi-reflection time-of-flight mass separator/spectrometer (MR-ToF MS) between the linear radio-frequency ion trap and the two Penning traps already in place. As a mass separator, the MR-ToF device has improved significantly ISOLTRAP's capability of purification of contaminated ion beams. In addition, the MR-ToF MS can be operated as a mass spectrometer, either to analyze the ISOLDE ion beam or for precision mass measurements of nuclides that are shorter-lived or that have lower yields than those accessible for Penning-trap mass spectrometry. The MR-ToF MS and corresponding components, its integration into ISOLTRAP, and its various operation modes are reviewed. Furthermore, a precision measurement of the $^{137}$Eu mass is presented, determined with the help of the MR-ToF device as a mass separator.


## 1. Introduction

The investigation of short-lived nuclides continues to contribute significantly to our understanding of nuclear structure, fundamental interactions and astrophysical processes [1–9]. The mass difference between an atom and the sum of its constituents, the total binding energy, reflects the sum of all their interactions. The differences in binding energy within isotopic and isotonic chains reveal the general structural evolution of atomic nuclei. In particular, they point to configurations of enhanced binding at so-called magic numbers. Other filters, like the empirical pairing gap, reveal more subtle changes in nuclear structure such as deformation, collectivity or residual proton-neutron interaction [10–18].

To understand the abundance distribution of the elements in our universe, a robust modeling of astrophysical processes which occur far from any earth laboratory is of major importance [19–21]. The mass, as the most fundamental ground state property, is among the most important input parameters for the reaction paths of nucleosynthesis, e.g. the *r* process [22–25], *rp* process [26–30], *s* process [31,32] and *νp* process [33,34].

A major step for precision mass spectrometry of short-lived nuclides was the introduction of the time-of-flight ion-cyclotron resonance (ToF-ICR) technique [35], pioneered with the ISOLTRAP experiment at ISOLDE–CERN over 20 years ago [36–39]. Here, ions of the radioactive species of interest are stored in a Penning trap to determine their cyclotron frequency $\nu = qB/(2\pi m)$, which is inversely proportional to their mass-over-charge ratio $m/q$ (and proportional to the magnetic field $B$). To achieve smallest mass uncertainties $\delta m$, the measurement has to be perturbation-free, in particular with respect to the Coulomb interaction with ions of other species, i.e. contaminations of the sample. Facilities like ISOLDE [40] produce a large variety of stable and unstable isotopes. These are usually mass-over-charge separated by magnetic separators before being sent to the experiments. The separators' mass resolving power on the order of $R = m/\Delta m = 10^3$ is sufficient to suppress neighboring isotopes, e.g. atomic ions with a different mass number $A = Z + N$, where $Z$ and $N$ are the number of protons and neutrons of the nucleus, respectively. However, usually one of the major challenges for subsequent experiments is the selection of the one ion of interest from the remaining isobaric ensemble, i.e. ions with the same number of nucleons. These contaminations may

* Corresponding author.
*E-mail address:* wolf@uni-greifswald.de (R.N. Wolf).

1387-3806/$ – see front matter © 2013 Elsevier B.V. All rights reserved.
http://dx.doi.org/10.1016/j.ijms.2013.03.020

originate from surface ionization in the hot environment of the target/ion source, like the atomic isobaric species in the case of alkali ions, or molecules formed in the ion source, e.g. oxides, fluorides, hydroxides, the so-called molecular sidebands. The required mass resolving power to suppress these isobars can vary from $R \approx 10^3$ up to $10^6$. Furthermore, investigations of isotopes far from stability are hindered by the steep decrease in production yield, alongside with a drop of half-life. This often reduces the abundance ratio between the ions of interest and the contamination ions. A fast and efficient removal of all contaminating species and the transfer of the ions of interest to the actual mass-measurement device is therefore of utmost importance for a successful experiment.

The MR-ToF mass separator/spectrometer (MR-ToF MS) is a recent development in time-of-flight mass analysis. Actually, a predecessor, the "Farvitron" [41], was introduced already in the early 1960s as a small high-vacuum gauge where electrostatic mirrors were used to periodically increase the density of a mass-over-charge specific ion bunch and to detect its mirror charge signal. However, it was not until 30 years later when Wollnik and Przewloka [42] described electrostatic time-of-flight mass spectrometers with multiple folded trajectories, see [43] for an overview. Due to their extended flight path which was no longer limited by the dimension of the device, long flight times could be achieved, leading to mass resolving powers several times higher than obtained up to then with table-top mass spectrometers. This property, combined with a fast operation cycle, single-shot measurement of several ion species (although of a limited mass range) and single-ion detection made the MR-ToF device appear as a promising mass spectrometer for short-lived species [44–46]. Furthermore, in combination with a fast ion selector, it was suggested to supply highly-resolved mass-over-charge selected bunches for subsequent experiments [47]. In the meantime, several of these systems are in operation or under construction [48–55].

Besides their applications related to mass-spectrometry, similar devices, often referred to as "electrostatic ion beam traps" (EIBT), are used for a wide range of atomic, molecular, and cluster studies [56–61]. In many cases the focus of EIBTs is not on their mass spectrometric aspects. Instead, they provide ion storage with the additional advantage of detection of neutral decay products.

In the following, the ISOLTRAP MR-ToF device will be reviewed. After its first successful on-line operation in 2010, the device has been applied in several different innovative experiments. The techniques and applications are presented, as well as preliminary results from on-line experiments.

## 2. Experimental setup and operation principle

Precision mass measurements with a sub parts-per-million (ppm) mass uncertainty utilizing a Penning trap demand a pure sample of one or at most a few ions of interest per measurement. The presence of a different species in the measurement trap leads to a perturbation of the individual mass-to-charge specific cyclotron frequencies due to Coulomb interaction, commonly referred to as space charge [62–66]. This is exemplified in Fig. 1 with ToF-ICR spectra of $^{229}Fr^+$ and $^{229}Ra^+$. In one case, about 40 ions of both species were simultaneously injected into the ISOLTRAP precision Penning trap with nearly equal abundances. In a second experiment, the $^{229}Ra^+$ions were removed by dipolar excitation prior to the ToF-ICR measurement of $^{229}Fr^+$. In the presence of the $^{229}Ra^+$ ions, there is a shift in the cyclotron frequency of $^{229}Fr^+$ of $\Delta\nu \approx 0.5$ Hz to lower values, i.e., higher mass, attributed to the Coulomb interaction between the two ion species. Furthermore, the cyclotron frequency of $^{229}Ra^+$ is shifted as well by about 0.4 Hz in the same direction. The relative difference of $\Delta\nu/\nu_c = 10^{-6}$ is about two orders of magnitude higher than the typical total uncertainty

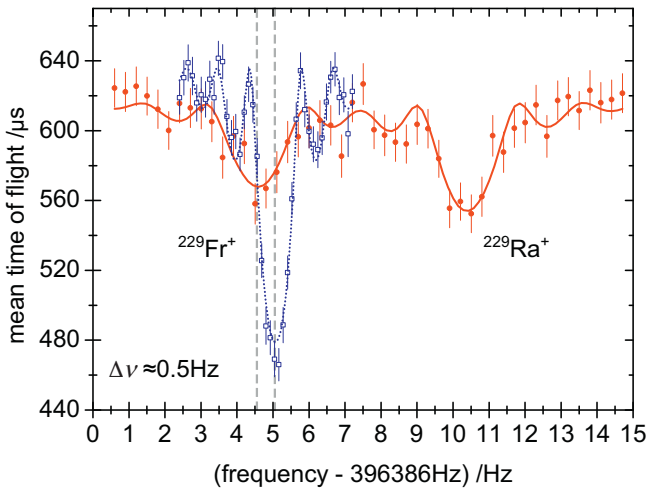


**Fig. 1.** Simultaneous ToF-ICR resonances, i.e., time of flight of ions ejected from the precision Penning trap as a function of excitation frequency, of $^{229}Fr^+$ and $^{229}Ra^+$ (red) and single-species resonance of $^{229}Fr^+$ (blue). In the first case, the cyclotron frequency of $^{229}Fr^+$ is shifted by almost $\Delta\nu \approx 0.5$ Hz to lower values, i.e., higher mass, due to Coulomb interaction in the Penning trap. The cyclotron frequency of $^{229}Ra^+$ is shifted by a comparable value in the same direction. About 40 ions where injected into the trap for each measurement step. In case of the double resonance, the excitation time was $T_{rf} = 0.6$ s, while for the single resonance, the excitation time was $T_{rf} = 1.2$ s. (For interpretation of the references to colour in this figure legend, the reader is referred to the web version of this article.)

achieved for measurements in the absence of space-charge effects. This example emphasizes the importance of contamination-free samples in Penning traps for precision measurements in the sub-ppm range.

For on-line experiments, besides the purity of the sample, the number of the ions delivered is an additional limiting factor. Short-lived nuclides with half-lives below a second, the usual measurement time of a Penning trap, are challenging due to the decay losses during the preparation and actual measurement. Therefore, the preparation time should be kept as short as possible. The MR-ToF mass separator combines high-resolution separation with a fast operation. It serves as a universal beam-composition analyzer and mass separator for species with half-lives down to a millisecond. Furthermore, it offers the possibility to use well-known species as simultaneous mass-markers, i.e., reference masses for MR-ToF mass measurements, which would be considered unwanted contaminants in the case of the Penning trap experiments.

### 2.1. Overview of ISOLTRAP

Before the implementation of the MR-ToF MS and corresponding components, the ISOLTRAP setup already included three ion-trapping devices: a segmented linear Paul trap (radio-frequency quadrupole (RFQ) cooler and buncher) in a horizontal beamline and two vertically installed Penning traps, each with its own superconducting magnet. Behind the RFQ, space was available for the installation of an additional MR-ToF MS device. Thus, this component had to be built to meet the restrictions of the already existing ISOLTRAP setup.

After the implementation of the MR-ToF MS, the experimental setup of ISOLTRAP, as shown in Fig. 2, currently includes four ion traps:

1. A helium buffer-gas filled RFQ cooler and buncher is used to accumulate the ions from ISOLDE and to convert the quasi-continuous beam to a pulsed beam [68]. The typical accumulation durations range from a few microseconds up to several hundreds of milliseconds, depending on the yield and half-life of

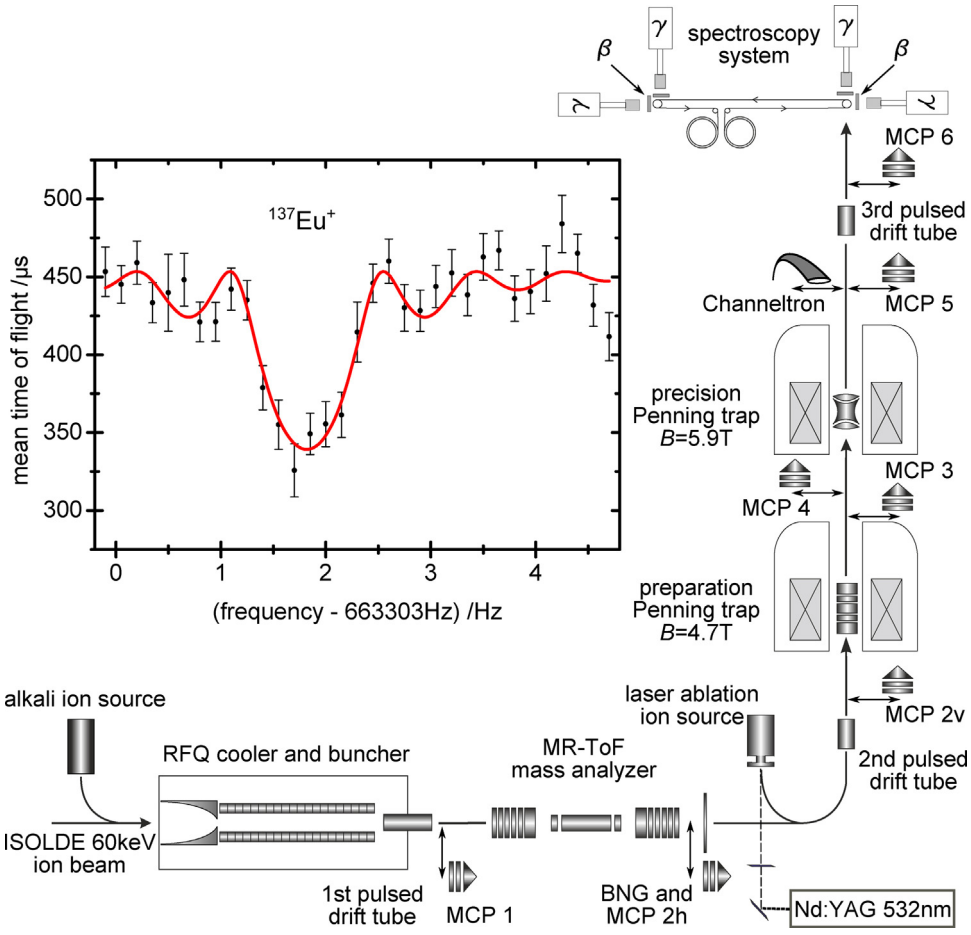


**Fig. 2.** Schematic overview of the ISOLTRAP setup (adapted from [67]). The inset shows a ToF-ICR spectrum of $^{137}Eu^{+}$. See text for further explanation.

the species. To thermalize the ions, a cooling period of around 10 ms is sufficient.

2. The MR-ToF MS can be used in combination with a Bradbury-Nielsen gate (BNG) as a fast ion selector [47,69] to separate the ions of interest from contaminations. Alternatively, it can be utilized in combination with an ion detector to directly observe the composition of the ion ensemble for mass spectrometry and other applications, which will be discussed below. The operation period for maximum mass resolving power of $R_{FWHM} \approx 200{,}000$ is about 30 ms.
3. A helium buffer-gas filled preparation Penning trap is used to further cool and mass-select the ions of interest [70] for the subsequent mass measurement in the precision Penning trap. The trap can be operated in cooling and bunching mode, only, at high gas pressures of about $10^{-3}$ mbar if the ion ensemble is already delivered essentially pure. The required centering can be accomplished in a few tens of milliseconds. For contaminated ensembles, mass-selective resonant buffer-gas centering is applied at typical pressures of about $10^{-4}$ mbar. The lower pressure is essential to achieve mass resolving powers in the order of $R = 10^5$. However, it also results in cooling periods of several hundreds of milliseconds, affecting the ion throughput and leading to losses in particular for ions with short half-lives.
4. The precision Penning trap, combined with a drift section in a magnetic-field gradient for time-of-flight measurements of the ejected ions, is used to determine their cyclotron frequency and thus their mass. To this end, the ion motion is probed by quadrupolar excitation at different frequencies (one at a time) to find the resonant conversion between magnetron and cyclotron motion. The increase in motional energy at the cyclotron frequency is detected by monitoring the ions' time of flight to a detector outside of the superconducting magnet. Dipolar excitation at the reduced cyclotron frequency can be applied prior to the actual mass measurement to clean the ensemble with mass resolving powers of up to $R = 10^6$.

In addition to the four ion traps, there are several supplementary devices. In particular, two off-line ion sources deliver the reference ions required for the calibration of the magnetic field: An alkali ion source in front of the RFQ produces potassium, rubidium and cesium ions. These ions are available to optimize the whole setup. A laser-ablation ion source located in front of the preparation Penning trap can be used to generate atomic or cluster ions by irradiating various bulk materials with 532-nm laser light [71]. Furthermore, a tape-station setup subsequent to the precision Penning trap has been installed for trap-assisted decay spectroscopy of isobarically and isomerically pure ion ensembles [72].

### 2.2. Details of the MR-ToF device

The MR-ToF mass analyzer, the BNG, a multichannel-plate (MCP) ion detector and adjacent ion optics were installed at ISOLTRAP in the CERN shutdown period 2009/2010. An ion-optical transfer section of about 1.8 m length in the horizontal ISOLTRAP beam line between the RFQ cooler and buncher and the laser-ablation ion source was used to accommodate the devices. A detailed description of the setup can be found in references [54,73]. It will only be summarized in the following.

The MR-ToF mass analyzer consists of two 160 mm-long electrostatic ion-optical mirrors, each incorporating six electrodes, surrounded by inner and outer shielding electrodes. The mirrors are separated by an 460 mm-long in-trap lift, a drift electrode whose electric potential can be pulsed to facilitate ion injection, ejection and control of the time-of-flight focus plane [74]. Ion species with different masses $m_i$, ejected from the RFQ at a potential $U$, gain the kinetic energy $E_{kin} = z_i eU = m_i v_i^2/2$, where $e$ is the elementary charge and $z_i$, $v_i$ are their charge state and velocity, respectively. Therefore, their time of flight $t_i$ for the same flight path is mass and charge dependent, $t_i \propto v_i^{-1} \propto \sqrt{m_i/z_i}$. Thus, they separate in time and can be resolved on an ion detector if their difference in time of flight $\Delta t_{ij}$ is larger than the individual signal widths $\Delta t_{i,j}$, $\Delta t_{ij} > \Delta t_{i,j}$.

High mass resolving power $R = m/\Delta m = t/(2\Delta t)$ can be achieved by either increasing the time of flight or decreasing the signal width at the detector plane. The latter is limited by the turn-around time of the ions in the ion source, i.e., depending on the ion velocity and the extraction field strength, and the Coulomb repulsion. The former can be increased by either reducing the average kinetic energy or extending the flight path. Decreasing the average kinetic energy $\bar{E}_{kin}$ leads to an increase in the relative kinetic energy spread $\delta_E = \Delta E_{kin}/\bar{E}_{kin}$, mostly unfavorable for the mass analyzer because the time-of-flight dispersion with respect to energy increases. Extending the flight path considerably is only possible by folding the flight path, i.e. the ions have to travel multiple times through the device. This technique is well known from, e.g. storage rings [5]. However, for high-resolution time-of-flight mass spectrometry, the successful application was shown just a few years ago [44–54]. Here, the individual species $i$ travel with $m_i/z_i$-specific revolution times $T_i \propto \sqrt{m_i/z_i}$. After $n$ revolutions, the time-of-flight difference of species $i$ and $j$ is grown by $\Delta t_{ij} = n\left|T_i - T_j\right|$, i.e. their separation increases linearly with the number of revolutions. By compensating time-of-flight dispersions with respect to the energy, angular and spatial distributions of the ions, the minimum signal width can be adjusted on the detector plane.

To store ions in an MR-ToF device, the potential maximum $U(x)$ inside a mirror has to exceed the ions' energy, i.e., their kinetic energy $E_{kin} < zeU(x)$ in the drift section. Injection and ejection from the MR-ToF device can be achieved by lowering the potential distribution of an ion mirror to a value that ions can pass the mirror without modifying the ions energy. An alternative approach is to use static mirrors and inject and eject the ions with a kinetic energy that exceeds the mirror potential maximum, $E_{kin} > zeU(x)$. The confinement can then be achieved by changing the ions' energy once they are between the mirrors. For this purpose, the in-trap lift has been introduced [74]. Furthermore, electrically switching the sensitive mirror potentials is avoided which reduces the electrical noise and fluctuations on the corresponding electrodes. The incoming ions have a kinetic energy $E_{kin}^{transfer} = zeU_{transfer} > zeU(x)$ that exceeds the maxima of the mirror potentials. Thus, they pass the first mirror and enter the activated in-trap lift electrode on a potential $U_{lift}$. While the ions travel through the electrode, it is switched to ground. Thus, the ions' energy is reduced to $E_{kin}^{trapping} = ze(U_{transfer} - U_{lift}) < zeU(x)$ and the ions are trapped. For ejection, the in-trap lift electrode is activated again while the ions are inside. Thus, they can pass the exit mirror for further transfer to the downstream experimental parts. The transfer energy in the horizontal beam line of ISOLTRAP is $E_{kin}^{transfer} \approx 3.1$ keV, while a trapping energy of $E_{kin}^{trapping} \approx 2.1$ keV is used for the MR-ToF mass analyzer. Furthermore, the in-trap lift can be used to maximize the mass resolving power. Depending on the ejection settings from the RFQ and the number of revolutions performed in the MR-ToF, the position of the time-focus plane changes. By modifying the kinetic energy of the ions inside the MR-ToF, i.e., changing $U_{lift}$, the position of the time-focus plane can be readjusted on the ion detector, as demonstrated in Fig. 3. This provides a simple and independent method to tune the mass resolving power, without changing the transfer energy outside the MR-ToF device or switching of the sensitive mirror voltages.

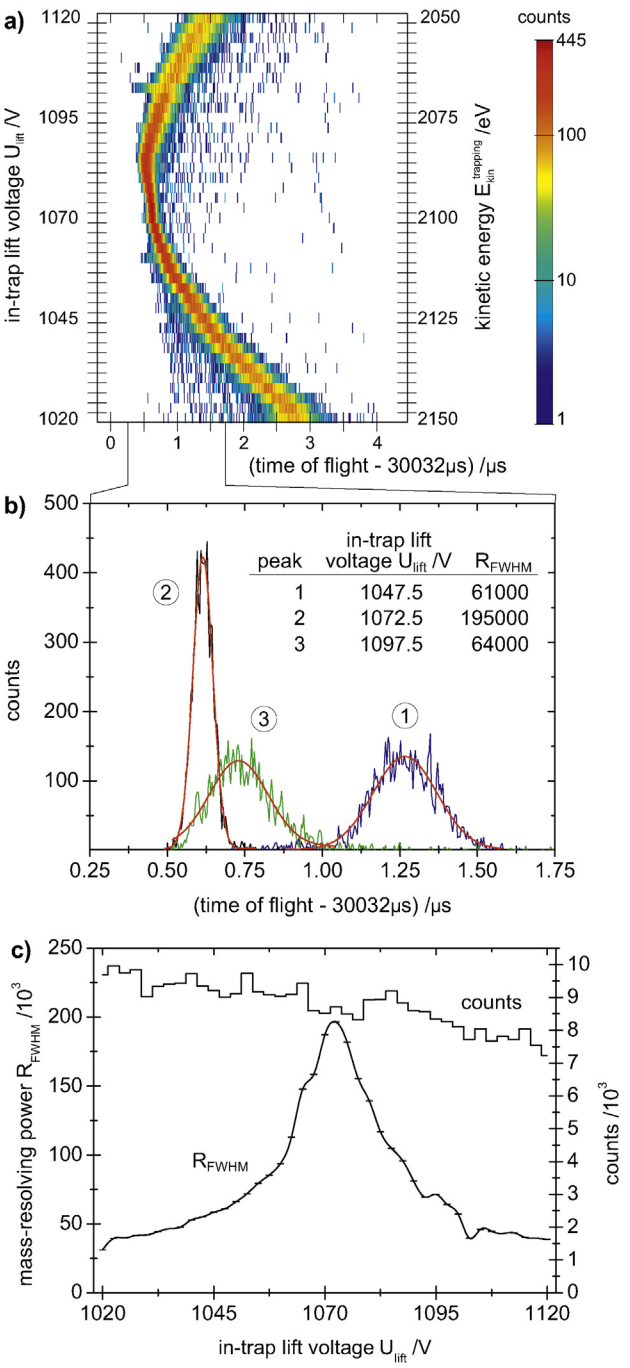


**Fig. 3.** In-trap lift time-of-flight focusing for $^{39}K^+$ ions at 2000 revolutions. (a) Color-coded number of counts as a function of the time of flight for different in-trap lift voltages and the corresponding kinetic energies. (b) Corresponding time-of-flight distributions for three in-trap lift voltages: the ToF focal plane is behind (peak 1), precisely at (peak 2) and in front of (peak 3) the detector. (c) Mass resolving power and number of integrated ion counts as a function of the in-trap lift voltage. A maximum mass resolving power of 200,000 is reached for about 1070 V.

The minimum separation in time needed to apply a selection with the BNG can be derived from its wire spacing [75] and the rise/fall times of the switches used to drive the two sets of wires. Suppression of an ion signal can be achieved if the transversal spread in beam radius (for a BNG in the "closed" state) is increased

sufficiently to not meet the acceptance of a subsequent aperture. This increase is determined by the wire distance, the voltage difference applied to neighboring wires, and the ions' energy. The voltage dependence sets an upper limit on the selection capabilities as shown in Fig. 10 of reference [54] due to the finite transmission even for closed BNG. Presently, the transmission of an unwanted species can be reduced by up to 4 orders of magnitude. Higher voltage differences would presumably increase the suppression factor, but have not been tested yet to avoid damaging the BNG.

### 2.3. Modifications of the RFQ

The RFQ buncher acts as an ion source for the MR-ToF device and the minimum bunch width provided by this source determines the time necessary to reach the maximum mass resolving power. Thus, the RFQ's trapping and ejection section has been modified to meet the MR-ToF requirements. The bunch width $\Delta t$ after MR-ToF MS trapping is a quadratic sum of the initial bunch width $\Delta t_0$ provided by the RFQ and contributions from the dispersion per turn, $\Delta T$, of the mass analyzer, $\Delta t = \sqrt{\Delta t_0^2 + (n\Delta T)^2}$. The mass resolving power

$$R = \frac{t}{2\Delta t} = \frac{t_0 + nT}{2\sqrt{\Delta t_0^2 + (n\Delta T)^2}} = \frac{t_0/n + T}{2\sqrt{\Delta t_0^2/n^2 + \Delta T^2}} \quad (1)$$

is, therefore, limited by the dispersion of the MR-ToF device, $R = T/2\Delta T$ for $n \to \infty$. In contrast, the initial bunch width determines the number of revolutions necessary to approach the maximum. It is limited by the turn-around time $\Delta t_0 = 2v_0 m/(qE_{ex})$ of the ions moving in the pulsed ion source (the RFQ), i.e. their velocity $v_0$ and the extraction-field strength $E_{ex}$ applied when the source is emptied [76]. This, in combination with the spatial distribution $\Delta x$ along the axis, determines the absolute energy spread, $\Delta E = E_{ex}\Delta x$. To decrease the initial time spread it is necessary to apply high extraction-field strengths. However, this increases the energy spread of the bunch. Therefore, to achieve low initial time spreads and low absolute energy distribution as well, an efficient cooling of the ion motion is required. This is accomplished in the RFQ by the application of a helium buffer gas. To decrease the spatial distribution, the RFQ trapping region was shortened. Originally, it had consisted of two segments with a total length of 20 mm (segments 24 and 25, see Fig. 4). This was modified by separating the two segments to form a trapping region of only 10 mm length. A dipolar extraction field is generated by switching the adjacent segments. By increasing the field strength from $E_{ex} \approx 3$ V/mm to $E_{ex} \approx 20$ V/mm, the bunch width on a detector in front of the MR-ToF device (MCP 1 in Fig. 2) was reduced from ≈900 ns to ≈60 ns for an ion-transfer potential of $E_{\mathrm{kin}}^{\mathrm{transfer}}/ez_i = 3.17$ kV, see Fig. 4. Thereby, the energy spread increased from about $\Delta E_{\mathrm{kin}}^{90\%} \approx 6$ eV to about $\Delta E_{\mathrm{kin}}^{90\%} \approx 60$eV. This results in a relative energy spread of $\delta_E^{\mathrm{trapping}} \approx 3\%$ at a trapping potential of $E_{\mathrm{kin}}^{\mathrm{trapping}}/ez_i = 2.1$ kV.

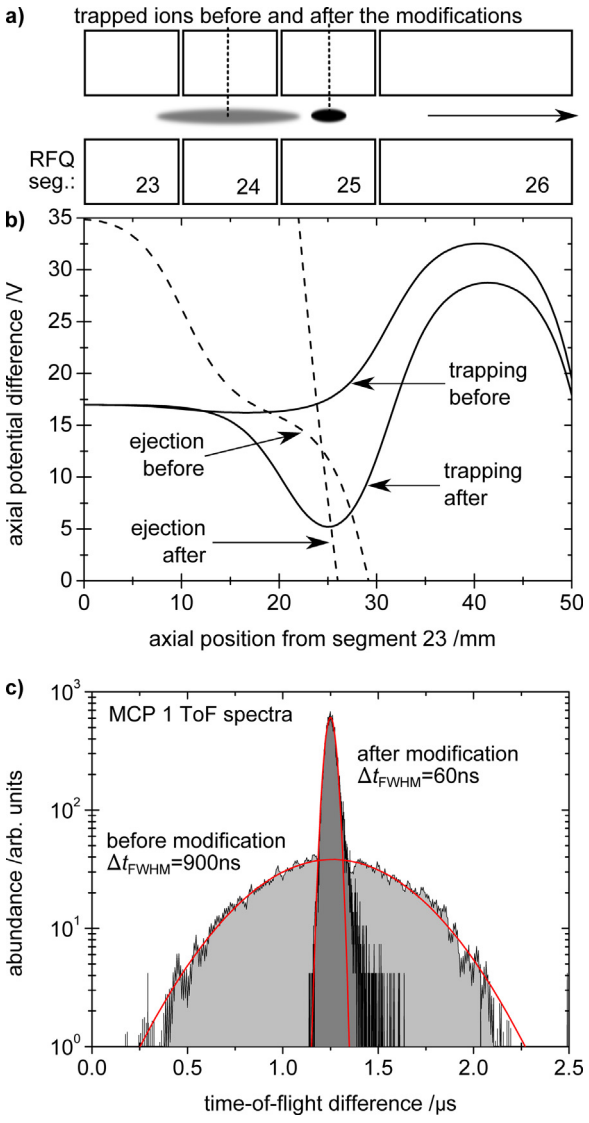


**Fig. 4.** Modification of the RFQ extraction section, properties before and after the intervention are shown. (a) Schematic illustration of the electrode configurations; (b) axial potential distributions for trapping and ejection; (c) time-of-flight distributions at MCP 1 (see Fig. 2).

## 3. Operation modes and applications

The MR-ToF mass analyzer has become a versatile tool for ISOLTRAP as well as for the ISOLDE facility. Originally intended as an auxiliary device to enhance the mass-purification capabilities for Penning-trap mass spectrometry (Fig. 5 bottom), it has additionally become a mass spectrometer in its own right, see (Fig. 5 top). Its advantage with respect to both mass separation and mass spectrometry lies in the combination of the following characteristics:

- fast measurement cycle, i.e., typically 30 ms, compared to Penning traps and therefore lower half-life limitations,
- high mass resolving power sufficient for most isobars, i.e., in excess of $10^5$,
- easy set up and fast operation readiness, e.g., less elements of the setup have to be prepared and optimized in preparation of a measurement campaign,
- non-scanning mode (in comparison to ToF-ICR): The whole (narrow-band, e.g. isobar) spectrum is obtained from a few injections. Contaminations are observed and identified simultaneously with the MR-ToF measurement, i.e. in the same mass spectra, and can even be utilized as calibrants,
- single-ion sensitive detection,
- contaminations do not perturb the measurement, as long as space-charge effects are avoided.

In the following some specific applications of the MR-ToF MS will be discussed in more detail.

### 3.1. Ion-beam analysis

The development and advancement of ionized rare-isotope beams continues to be a major issue at on-line facilities like ISOLDE,

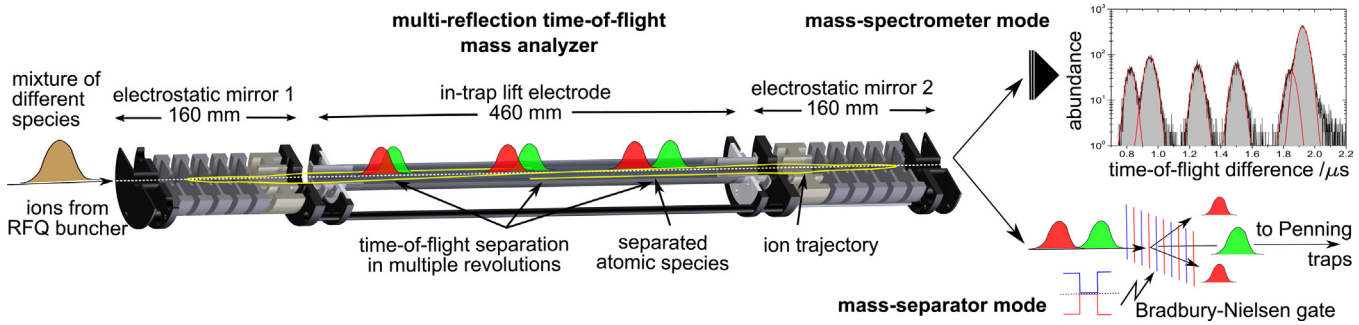


**Fig. 5.** Sectional view (adapted from [54]) of the MR-ToF device. The mass-separated ions are either detected by a microchannel-plate detector to record a time-of-flight spectrum (right top) or selected by the BNG (right bottom).

see e.g. [77,78]. A prerequisite is the qualitative and quantitative analysis of the ion-beam composition, influenced by e.g., rare-isotope production cross sections, ionization efficiencies, and time structure, e.g. effusion and diffusion flux, and half-lives of the isotopes.

The time-of-flight spectra obtained with the MR-ToF mass analyzer and an ion detector can be used to analyze the composition of unknown ion beams. For this purpose, the ToF spectrum has to be converted into a mass spectrum. This is achieved by the use of well-known calibrant ions, which connect mass and time of flight with respect to a set of operation parameter of the mass analyzer. In general, for a rough identification of nuclear species, an "external", i.e. non-simultaneous, calibration with two or more different ion species, e.g., with stable isotopes from the alkali ion source, is sufficient. This allows assigning a mass-over-charge value, and therefore a likely species, to every flight time. As a start, if one species in the spectrum is clearly identified, the relative distances to the neighboring time-of-flight signals can be used to further analyze the ensemble. This procedure is advantageous in case of voltage drifts, e.g., due to a change in the environmental conditions, which might cause time-of-flight deviations. While these may shift the absolute positions of the peaks, the changes in the distances between close-neighboring signals remain negligible.

In cases where ISOLDE's resonance-ionization laser ion source (RILIS) [79] is employed, the unambiguous identification of one of the unknown ions in the time-of-flight spectrum can easily be accomplished: The RILIS system can be tuned to selectively ionize only the species under investigation. Blocking the laser beam leads to an immediate drop of the signal of the corresponding ion in the time-of-flight spectrum, i.e. a straightforward identification, as shown for $^{185}Au^{+}$ in Fig. 6: The surface-ionized isobar $^{185}Tl^{+}$ is well separated after a flight time of about 33 ms. By monitoring the count rate the ionization efficiency can be optimized even for very low yields, independent of branching ratio and half-life, as described below. Furthermore, the hyperfine structure of the isotope under investigation can be studied by scanning of the resonances, as show in Fig. 7 as a proof of principle with a relatively large laser line width [80]. A high count-rate range of four orders of magnitude could be recorded background free. A detailed discussion about the application of the MR-ToF MS in the field of in-source laser spectroscopy is out of the scope of the present treatment and will be given elsewhere [81].

The abundance ratios of the different species composing the MR-ToF time-of-flight spectrum are in many cases a direct representation of the ion-beam composition delivered from ISOLDE. Depending on the isotope, corrections may have to be applied with respect to, e.g., the half-lives and charge-exchange rates from collisions with buffer-gas atoms in the RFQ. By varying the delay between the ISOLTRAP RFQ collection-time window and the proton irradiation pulse on the ISOLDE target, the time structure of the release of the nuclides from the target can be sampled. To derive absolute yield numbers, the efficiency of the ISOLTRAP setup up to the MR-ToF MS can be calibrated by the signal intensity of a reference beam.

Currently, the intensity of an ion beam from ISOLDE is monitored with Faraday-cups, which give only an integral number and no information on the composition. In addition, the sensitivity on the order of picoamperes is not sufficient to measure the yield of very exotic species far away from the valley of stability. The beam composition is determined by nuclear decay spectroscopy. This method, however, comes to its limits if the half-life exceeds a few tens of seconds, if the branching ratio is unfavorable (as, e.g., in Fig. 7, with an $\alpha$-decay branching fraction of $^{185}$Au of only 0.26%), or if the production in the target is low. In contrast, the MR-ToF MS offers an efficient alternative to both Faraday-cup beam-current measurement as well as decay spectroscopy as it has no intrinsic upper half-life limit, provides single-ion counting and can distinguish the species delivered by its ultra-high mass resolving power. Thus, the MR-ToF MS is a universal analytical tool that provides yield information for stable to short-lived species down to the 10-ms half-life range.

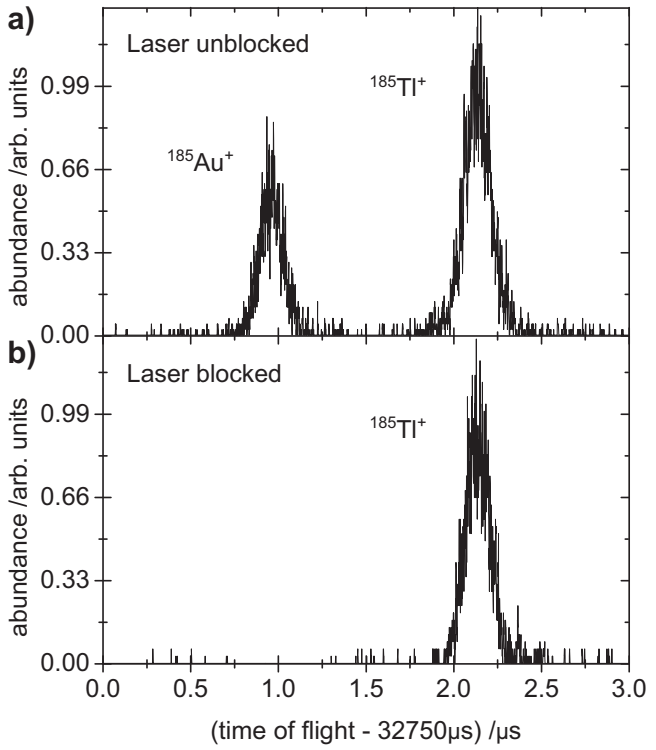


**Fig. 6.** $A = 185$ time-of-flight spectra after 1000 revolutions in the MR-ToF MS. (a) The RILIS lasers were tuned to ionize $^{185}Au^{+}$ atoms. The clear separation from $^{185}Tl^{+}$ isotopes enables a background-free gold-yield analysis. (b) Furthermore, blocking the laser beam unambiguously identifies the gold isotope.

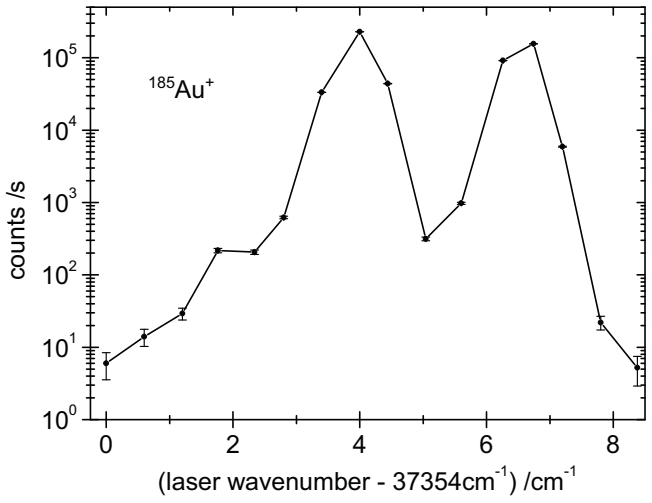


**Fig. 7.** Signal intensity of $^{185}Au^+$ (scaled to RFQ accumulation time of 1 s), representing the ionization efficiency, as a function of the wavenumber of the RILIS first excitation step ($6^2S_{1/2} \rightarrow 6^2P_{1/2}$; the two resolved resonances of the hyperfine-structure correspond to the transitions $F$=3 → 2,3 (left peak) and $F$=2 → 2,3 (right peak)). The laser line width was 0.33 cm$^{-1}$.

The ion-identification capability can be used to optimize the ISOLDE performance for particular experimental requirements, e.g., to find the best parameters to enhance or suppress the yield of specific isotopes. For example, the temperature of an ISOLDE target determines the diffusion time of the ions out of the target. In Fig. 8, the target temperature was varied from about 1740 °C to 1810 °C and the effect on the ion ensemble was observed with the MR-ToF MS: At mass $A$ = 72 the spectrum shows, amongst others, the short-lived ions $^{72}Ga^+$ and $^{72}Cu^+$, with half-lives of 14.10(2) h and 6.63(3) s, respectively [82]. The proposed species are the ones with the best-matching flight times. In the case of close matches, additional arguments are taken into account, such as target material, production mechanism and associated cross sections. One can clearly see in Fig. 8 that the copper yield increases by a factor of two due to faster diffusion whereas the number of counts of the contaminating isotopes stays the same. It is noteworthy, that even the $^{40}Ca^{32}S^+$ signal can be evaluated although it is only a shoulder of the dominant $^{72}Cu^+$ peak.

### 3.2. Ion-beam purification

The first successful on-line application of ISOLTRAP's MR-ToF mass separator was during mass measurements of neutron-rich argon isotopes in July 2010. The MR-ToF MS was used in addition to the preparation Penning trap to purify $^{45}Ar^+$ ions from contaminations, mainly consisting of molecules delivered from ISOLDE. An on-line operation resulting in a new mass value was just two months later: In the rare-earth region at $A$=137, the mass of $^{137}$Eu could be measured for the first time. Here, the MR-ToF was used again as an auxiliary purifier in combination with the preparation Penning trap. Contaminations of isobaric barium, praseodymium, neodymium, promethium and samarium were present in the ISOLDE beam (see Fig. 12 in [54]). The MR-ToF MS resolved these species with a flight time of about 22 ms. The signal of $^{137}Eu^+$ was not visible in the spectrum due to the low dynamic range of the transient recorder used for data acquisition during the first MR-ToF MS experiments. At this early time, the BNG could suppress the contaminants by only a factor of 10, since only small deflection voltages were applicable. However, the suppression was still essential for the success of this measurement. Three resonances could be recorded, one with $T_{rf}$ = 0.1 s and two with $T_{rf}$ = 1.2 s excitation time. In total 1678 ion events were recorded. $^{133}Cs^+$ from the

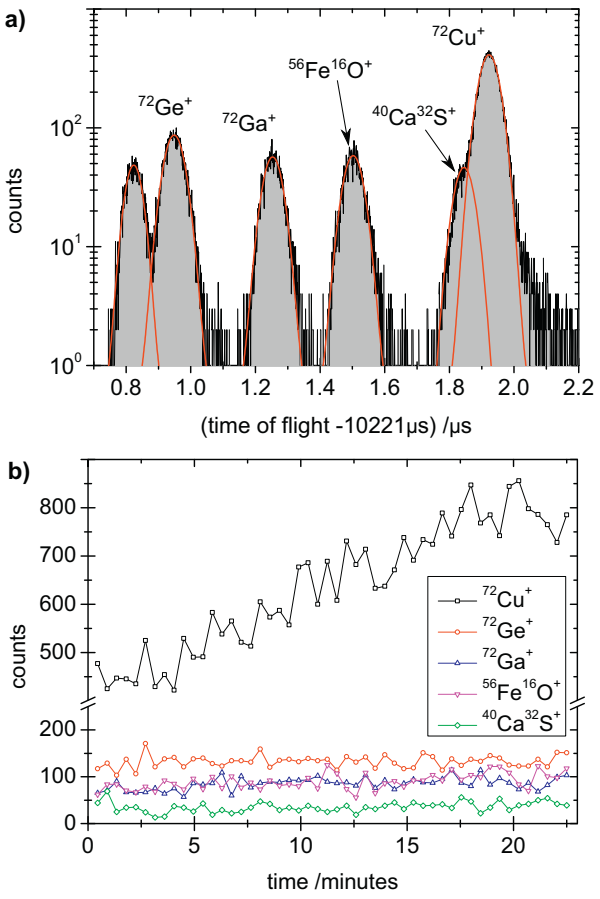


**Fig. 8.** (a) Integral time-of-flight spectrum for $A$ = 72 as delivered from ISOLDE during heating of the target material; (b) number of ion counts of the isotopes from the spectrum above as a function of the time during increase of the target heating by approximately 70 °C.

off-line alkali ion source served as a reference. From the mean frequency ratio, derived from a standard evaluation procedure [83], $r = \nu^{ref}_{133Cs}/\nu_{137Eu} = 0.970570108(35)$, the mass excess is determined to be $ME(^{137}Eu)_{ISOLTRAP} = m(^{137}Eu) - A$ u = −60145.87(4.28) keV/c$^2$, where $A$ is the mass number and u the unified atomic mass unit. The relative mass uncertainty of $\delta m/m = 3.5 \times 10^{-8}$ is dominated by the statistical uncertainty of the cyclotron frequencies. With a difference of $\Delta ME(AME2012 - ISOLTRAP) = 25.87$ keV/c$^2$ this agrees well with the extrapolated AME2012 [84] value of $ME(^{137}Eu)_{AME2012} = -60120\,\#\,(200\,\#)$keV/c$^2$.

As described above, the MR-ToF mass separator and the BNG can be used as an auxiliary mass purifier in combination with the preparation Penning trap. Furthermore, the system has been used as the only mass separator while the preparation Penning trap served as an ion accumulator and cooler. The conditions favoring one of these two operation modes depend on the half-lives of the species to be investigated, yields of the contamination ions, suppression ratios of the contamination, and mass resolving power necessary.

If the half-life of the ion of interest is comparable to, or less than, the usual separation period of the preparation Penning trap, i.e. 300 ms, ion losses due to decays reduce the efficiency of ISOLTRAP as a whole. In this case, using the MR-ToF mass separator as the only purifier is favorable because of its fast separation cycle, in the range of a few 10 ms. The preparation Penning trap is then used just for re-bunching of the selected species in a high buffer-gas environment, which is typically achieved in a few 10 ms as well. This scheme has been applied, e.g., for the mass measurement of the short-lived isotope $^{82}$Zn [85] with a half-life of 228(10) ms [86],

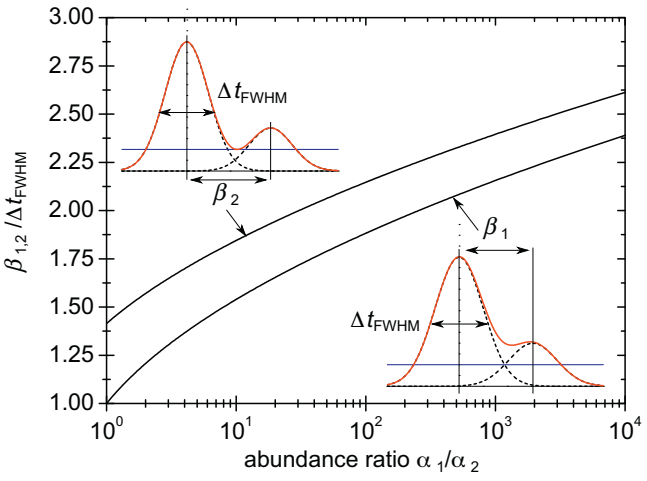


**Fig. 9.** Necessary increase $\beta$ in peak separation, i.e. mass resolving power, as a function of the abundance ratio $\alpha_1/\alpha_2$ of two species. The curves are given exemplarily for two cases where the individual signals are separated to a distance $\beta_{1,2}$ as shown in the insets. In the case of $\beta_1$, both species are separated to a distance where the more abundant signal has decreased to the half-height of the less abundant signal (blue line). In the case of $\beta_2$, the summed signal (red curve) has decreased to the half-height of the less abundant signal. Both signals are assumed to be Gaussian shaped, with the same $\Delta t_{FWHM}$. (For interpretation of the references to colour in this figure legend, the reader is referred to the web version of this article.)

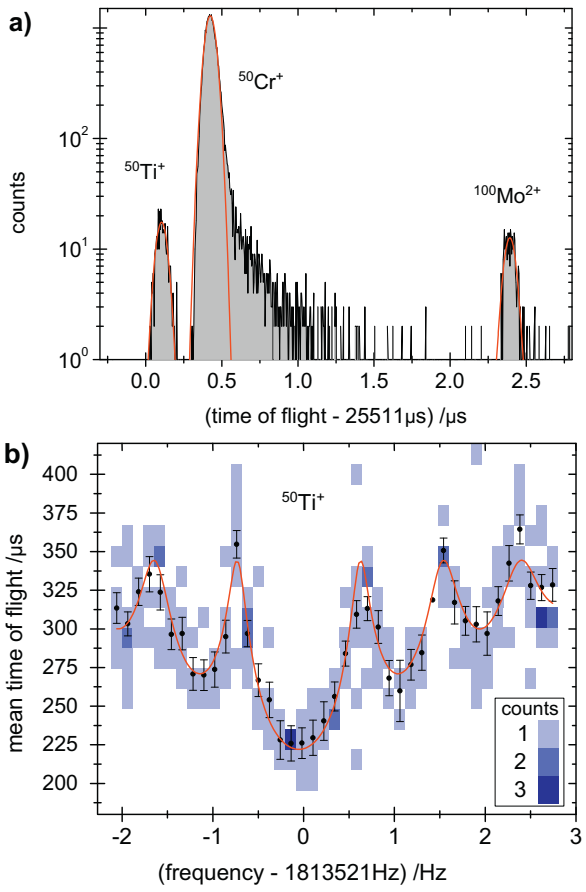


**Fig. 10.** (a) MR-ToF mass spectrum of $A = 50$ isobars at 1500 revolutions, showing $^{50}Ti^+$, $^{50}Cr^+$ and $^{100}Mo^{2+}$. (b) ToF-ICR measurement of $^{50}Ti^+$ with $T_{rf} = 1.2$ s excitation time, only 300 ions recorded. The much more abundant $^{50}Cr^+$ contamination has been removed and simultaneously the number of detected $^{50}Ti^+$ per second has been increased by a factor of 10, see text for explanation.

that could be separated from the contaminating $^{82}$Rb and prepared for the mass measurement in less than 25 ms.

The suppression achievable by the MR-ToF mass separator and the BNG is limited by the distributions of the time-of-flight signals and the deflection angle of the BNG. The time-of-flight distribution of different species, i.e. their separation in time at a given height of the signal, is limited by the maximum mass resolving power. Furthermore, asymmetric peak shapes, large tails, and unfavorable abundance ratios between the species will limit the contamination suppression. For Gaussian-shaped time-of-flight signals, the required increase $\beta(\alpha_1, \alpha_2)$ in mass resolving power, i.e., $R_\beta = \beta \cdot R_{FWHM}$, as a function of abundance ratio $\alpha_1/\alpha_2$ is shown in Fig. 9.

For asymmetric ToF distributions, the suppression depends also on whether the ion of interest is on the high-mass side or on the low-mass side of the contaminant, see for example Fig. 10. Here, the contaminant $^{50}Cr^+$ has a tailing edge below the 5%-intensity level of the high-mass side. A clean mass selection of an ion of interest on this side would not be possible. Therefore, in practice, the separation of multiple species and consequently their purification depends strongly on the peak shapes, their abundance ratio and the difference in mass.

For ions of interest with half-lives reasonably longer than the usual separation period of the preparation Penning trap, both devices can be used in combination to increase the accessible contamination to ion-of-interest ratio. This is preferable if the separation by the MR-ToF/BNG combination is hampered by large abundance differences.

Another operation mode in the case of heavily contaminated ion beams is the repeated MR-ToF MS application and accumulation of the ion bunches delivered from the MR-ToF separator in the preparation Penning trap. Due to the limited measurement time available in an on-line experiment, it is desirable to have on average at least one ion of interest processed by the measurement trap per cycle. If the ratio between contaminants and ions of interest is too high, the total number of simultaneously mass-separated ions required to provide at least one purified ion of interest can be so large that space-charge effects due to Coulomb interactions inhibit the MR-ToF MS from separating the different species [87,88]. This effect is known as peak coalescence, but a detailed evaluation with respect to the corresponding conditions is not yet available. Therefore, in practice the number of ions in the MR-ToF has to be increased with care. The maximum number of ions that can be handled by the MR-ToF MS depends on the mass difference and abundance ratio of the species of interest and the contaminations. Typically, it is in the order of only some hundreds up to several thousands. However, when the half-life of the ion of interest is sufficiently long (about a second or more), the number of available ions per mass-measurement cycle in the precision trap can be increased significantly by repetitive injections of mass-selected bunches from MR-ToF MS into the preparation Penning trap. In this case, the preparation Penning trap acts as an accumulator to capture the mass-selected species of interest, ejected from the MR-ToF MS in intervals of some ten milliseconds. Therefore, the available number of ions for a subsequent mass measurement increases in principle linearly with the number of injections, while the overall increase in cycle time is comparably low. If the contamination is too strong and exceeds the suppression limits of the MR-ToF MS, or the accumulated ions get significantly contaminated by their own decay products, a final cleaning process in the preparation Penning trap can be applied before the transfer to the precision Penning trap is performed. With a contamination suppression of $10^4$ by the BNG (see above) and an additional cleaning process in the preparation Penning trap removing another two orders of magnitude of contamination, ratios of up to $10^6$ contaminating ions to ions of interest can be handled.

Alternatively, if the purification by the MR-ToF MS is sufficient and the decay of accumulated ions is not critical (decay products not trapped or sufficiently long half-life of ion-of-interest), additional cleaning in the preparation Penning trap is not required. To save measurement time, only cooling and bunching with a high buffer-gas pressure and a permanent quadrupolar excitation is applied. This accumulation scheme has been used with up to 50 injections, where the resulting number of separated ions for the mass measurement scaled with the number of injections.

Fig. 10 shows a ToF-ICR test measurement of stable $^{50}Ti^+$ ions, which were contaminated with a 74 times higher yield of $^{50}Cr^+$ ions. A separation time of about 25 ms has been used to achieve a resolving power of $R_{FWHM} \approx 150000$, whereas the time-of-flight difference is 278 ns since the mass difference is 1.17 MeV/c$^2$. The ISOLDE beam was accumulated for 80 ms in the RFQ, which resulted in an average count rate of about 1.6 $^{50}Cr^+$ per mass-measurement step in the precision Penning trap. The count rate for $^{50}Ti^+$ was too low to perform a measurement within an adequate time. Thus, the number of accumulations in the preparation Penning trap was increased from 1 to 30, the average count rate of $^{50}Ti^+$ in the precision Penning trap could be increased to 0.65 per measurement step. The measurement period for a $T_{rf} = 1.2$ s excitation time ToF-ICR increased by a factor of 3 from 1.7 s (including all other experimental steps) to about 5 s (this includes additional 29 accumulation steps consisting of 80 ms RFQ accumulation, 10 ms RFQ cooling and 25 ms MR-ToF mass separation, thus 3.335 s). In summary, the increase in count rate was a factor of 30, while the measurement time increased by just a factor of 3, which amounts to a 10-fold reduction of on-line time to obtain a ToF-ICR measurement of $^{50}Ti^+$. This has been achieved without increasing the space charge in the MR-ToF MS and is therefore a suitable method to tackle high contamination-to-ion-of-interest ratios. As can be seen in Fig. 10, the individual time-of-flight distribution of the ions for each frequency step of the radio-frequency excitation scan show that there are no contaminants "leaking" into the resonance (these would assemble at flight times around 350 μs, independent of the frequency).

The total on-line measurement time (typically limited to few hours per nuclide) plays an important role for experiments with rare ion beams with only a few ions of interest per second. A more detailed description of this important method is out of the scope of the present article. It will be presented in a forthcoming publication [89].

### 3.3. MR-ToF precision mass spectrometry

The possibilities for precision mass spectrometry of exotic isotopes are limited with respect to half-life and yield of the ion of interest. As a consequence, this limits observation time $t$ and the number of ions $N$ detectable within an on-line experiment. For conventional Penning-trap mass spectrometry, the mass resolving power [90] $R = \frac{m}{\Delta m} = \frac{\nu_c}{\Delta \nu_c} \approx 1.25 \nu_c t$ increases linearly with the observation time and can reach millions. For MR-ToF devices, the mass resolving power given in Eq. (1) reaches a maximum value when the growth in time-of-flight dispersion per revolution is nearly linear. Fig. 11 compares the conventional Penning-trap mass resolving power of ISOLTRAP ($B = 5.9T$) with that of its MR-ToF MS for a typical ion ($\nu_c = 1$ MHz, e.g. $A/z \approx 90$). For isotopes with very short half-lives, i.e., below 100 ms, the mass resolving power of the MR-ToF MS is up to an order of magnitude higher than for the Penning trap. This favors the MR-ToF device as a mass separator and, regarding the statistical mass uncertainty, $\delta m/m \propto (R\sqrt{N})^{-1}$, also as a mass spectrometer, over the Penning trap [53]. However, recent developments in Penning-trap mass spectrometry have potentially extended the limits of the latter [91,92,93].

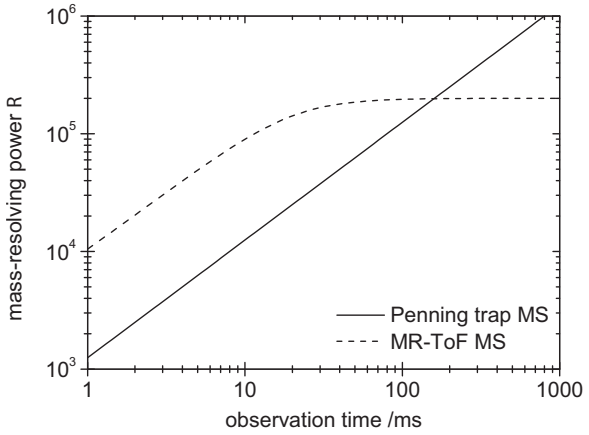


**Fig. 11.** Mass resolving power as a function of the observation time for ISOLTRAP's precision Penning trap ($B = 5.9T$) and MR-ToF MS for a typical ion of $A/z \approx 90$.

As already described in Section 3.1, unknown isotopes and molecules can be identified by performing a time-of-flight calibration of the instrument. The ion's time of flight is connected to its mass-over-charge ratio by the general relation

$$t = a\sqrt{\frac{m}{ze}} + b, \quad (2)$$

where $a$ and $b$ are device-specific parameters. The parameter $a$ increases with the trapping time in the MR-ToF MS (number of revolutions the ions undergo in the device), while the parameter $b$ is independent of it. To determine the two parameters $a$ and $b$, at least two independent reference measurements have to be performed. This can involve either two calibrant ions with known masses or – if only one such reference ion is available – by performing measurements with at least two different numbers of turns in the MR-ToF device.

In addition, two types of calibrant ions can be distinguished, "internal" and "external". Internal calibrants are the ones, which are recorded, in the same time-of-flight spectrum as the ion of interest. They are typically isobaric species delivered by the same ISOLDE ion beam. External calibrants are the ones which belong to different time-of-flight spectra than that of the ion of interest. They are typically ions from the off-line ion source. The two methods as well as a combination of internal and external calibrants are described briefly in the following.

The ideal situation for an MR-ToF mass measurement, from the point of view of the systematic errors, is the availability of a fully internal calibration with two or more simultaneously detected species with well-known masses. The advantage is that all species encounter the same fluctuations in time of flight, which may come from changes in the mirror potentials or other drifts in the setup. The fluctuations can be monitored through recording time-of-flight spectra in short measurement intervals, as shown in Fig. 12. Data that was collected in this way can now be corrected for systematic fluctuations. The reference ions can act in each individual spectrum as anchor points from which the time-of-flight differences to the ion of interest can be evaluated. Therefore, the calibration is practically free of systematic errors originating from time-varying fluctuations and drifts of the spectrometer parameters. The data from Fig. 12 was used to create Fig. 8. Again, the increasing copper yield can be seen.

In the case that only one reference species accompanies the ion of interest, two methods can be applied to obtain the calibration and therefore the mass. Either the spectrum is measured at two different flight times, i.e. two different numbers of revolutions in the MR-ToF MS, or at least one additional ion species is employed as an external calibrant. The former method uses the fact that the

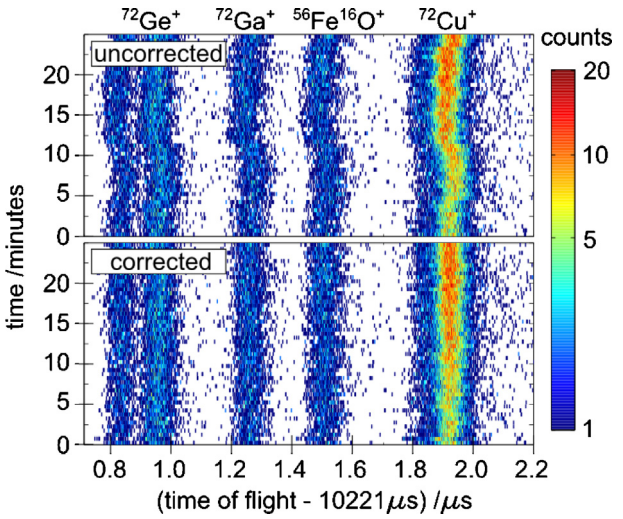


**Fig. 12.** 2D color-coded intensity plot of time-of-flight spectra of $A = 72$ isobars, i.e. the number of ion counts as a function of time of flight on abscissa and as a function of measurement time on the ordinate. The uncorrected time-of-flight data (top) can be corrected (bottom), in this particular case with respect to the $^{72}Ge^+$ signal, in order to sum up all events in one spectrum, as shown in Fig. 8 (see text for further explanations).

parameters $a$ and $b$ can be eliminated from Eq. (2) by subtracting the time of flight times of two different revolution numbers. Thus, the mass of the ion of interest can be determined by only the time differences and the mass of the one internal reference ion. The alternative method uses an external calibrant, which has to be provided from, e.g., an off-line ion source. In all other respects, like the preparation in the RFQ, it is treated in the same way as the ion of interest. In particular, the external time-of-flight reference is measured at the same number of revolutions. This measurement is performed both immediately before and after the data of the ion of interest are taken.

The least convenient situation is the absence of internal calibrants. In this case, these have to be provided externally. As in all cases were a second time-of-flight spectrum is needed to complete a mass measurement, the spectra have to be measured in short alternating periods to reduce systematic drifts as much as possible.

Tests of these mass-measurement methods over a wide mass range have shown that – for the cases were at least one internal reference is available – the achievable relative uncertainty is in the ppm to sub-ppm region. First MR-ToF precision mass measurements of short-lived nuclides and a detailed discussion of the statistical and systematic uncertainties of the respective methods are beyond the scope of the present discussion and will be provided in future publications (ref. [94] and [95] respectively).

## 4. Conclusion and outlook

Three years after its implementation, the MR-ToF MS is a well-established enhancement of the ISOLTRAP mass spectrometer. Its performance as a mass purifier has increased the range of rare isotopes that is accessible for precision mass spectrometry. Due to the reduced time required to reach high mass resolving powers, the MR-ToF MS became the method of choice for the purification of short-lived isotopes, while the preparation Penning trap still serves as a specialized device for accumulation and cooling.

The MR-ToF MS application as a precision mass spectrometer of its own right for very short-lived species was recently tested successfully. It opens new regions of the chart of nuclides for future measurement campaigns as the experimental cycles are shorter and the required ion yields are smaller than that required for Penning-trap mass measurement. In addition, what used to be unwanted contaminants producing space-charge shifts in the case of ICR measurements are now exploited as mass markers, i.e. provide reference mass values. By monitoring the corresponding reference-ion signals a simultaneous calibration is performed which significantly reduces the uncertainty due to temporal fluctuations.

In addition to its use for beam purification as a preparatory step before the Penning-trap mass measurement and its application as a precision mass spectrometer itself, the MR-ToF MS can supply important information for the target and ion-source developments at ISOLDE. Unambiguous identification of unknown species, e.g. molecular ions as isobaric contaminants of the ions of interest, and background-free yield analysis independent of decay spectroscopy, e.g. also suitable for long-lived species, will simplify and enhance the optimization of the on-line isotope-separator facility at CERN and the characterization of new developments.

## Acknowledgements

This work was supported by the German Federal Ministry for Education and Research (BMBF) (Grants No. 06GF9102, 05P12HGCI1, 05P12HGFNE and 06DD9054), the Max-Planck Society, the IMPRS-PTFS, the European Union seventh framework through ENSAR (Contract No. 262010), the French IN2P3 and the Nuclear Astrophysics Virtual Institute (NAVI) of the Helmholtz Association. We acknowledge the support of the ISOLDE Collaboration and technical teams.

## References

[1] D. Lunney, J.M. Pearson, C. Thibault, Reviews of Modern Physics 75 (2003) 1021–1082.
[2] K. Blaum, Physics Reports 425 (2006) 1–78.
[3] L. Schweikhard, G. Bollen, International Journal of Mass Spectrometry 251 (2–3) (2006) 85.
[4] J. Äystö, Nuclear Physics A 805 (2008) 162c–171c.
[5] B. Franzke, H. Geissel, G. Münzenberg, Mass Spectrometry Reviews 27 (2008) 428–469.
[6] K. Blaum, J. Dilling, W. Nörtershäuser, Physica Scripta 2013 (2013) 014017.
[7] M. Block, Direct mass measurements of the heaviest elements with Penning traps, in this issue.
[8] R. Ringle, S. Schwarz, G. Bollen, Penning Trap Mass Spectrometry of Rare Isotopes Produced Via Projectile Fragmentation at the LEBIT Facility, in this issue.
[9] J. Dilling et al., in this issue.
[10] A. Jensen, P. Hansen, B. Jonson, Nuclear Physics A 431 (1984) 393–418.
[11] J.-Y. Zhang, R. Casten, D. Brenner, Physics Letters B 227 (1989) 1–5.
[12] I. Talmi, Reviews of Modern Physics 34 (1962) 704–722.
[13] P. Federman, S. Pittel, Physics Letters B 69 (1977) 385–388.
[14] P. Federman, S. Pittel, Physics Letters B 77 (1978) 29–32.
[15] K. Heyde, P.V. Isacker, R. Casten, J. Wood, Physics Letters B 155 (1985) 303–308.
[16] R.B. Cakirli, D.S. Brenner, R.F. Casten, E.A. Millman, Physical Review Letters 94 (2005) 092501.
[17] D. Neidherr, G. Audi, D. Beck, K. Blaum, C. Bohm, M. Breitenfeldt, R.B. Cakirli, R.F. Casten, S. George, F. Herfurth, A. Herlert, A. Kellerbauer, M. Kowalska, D. Lunney, E. Minaya-Ramirez, S. Naimi, E. Noah, L. Penescu, M. Rosenbusch, S. Schwarz, L. Schweikhard, T. Stora, Physical Review Letters 102 (2009) 112501.
[18] R.B. Cakirli, R.F. Casten, in this issue.
[19] H. Schatz, et al., in this issue.
[20] S. Goriely, et al., in this issue.
[21] S. Kreim, M. Hempel, D. Lunney, J. Schaffner-Bielich, Nuclear masses and neutron stars, in this issue.
[22] M. Arnould, S. Goriely, K. Takahashi, Physics Reports 450 (2007) 97–213.
[23] S. Baruah, G. Audi, K. Blaum, M. Dworschak, S. George, C. Guenaut, U. Hager, F. Herfurth, A. Herlert, A. Kellerbauer, H.-J. Kluge, D. Lunney, H. Schatz, L. Schweikhard, C. Yazidjian, Physical Review Letters 101 (2008) 262501.
[24] S. Goriely, A. Bauswein, H.-T. Janka, ApJL 738 (2011) L32.
[25] G. Savard, J. Clark, in this issue.
[26] H. Schatz, A. Aprahamian, J. Gorres, M. Wiescher, T. Rauscher, J.F. Rembges, F.K. Thielemann, B. Pfeiffer, P. Moller, K.L. Kratz, H. Herndl, B.A. Brown, H. Rebel, Physics Reports 294 (1998) 167–263.
[27] H. Schatz, A. Aprahamian, V. Barnard, L. Bildsten, A. Cumming, M. Ouellette, T. Rauscher, F.K. Thielemann, M. Wiescher, Physical Review Letters 86 (2001) 3471–3474.
[28] D. Rodriguez, V.S. Kolhinen, G. Audi, J. Äystö, D. Beck, K. Blaum, G. Bollen, F. Herfurth, A. Jokinen, A. Kellerbauer, H.J. Kluge, M. Oinonen, H. Schatz, E. Sauvan, S. Schwarz, Physical Review Letters 93 (2004) 161104.

[29] M. Breitenfeldt, G. Audi, D. Beck, K. Blaum, S. George, F. Herfurth, A. Herlert, A. Kellerbauer, H.J. Kluge, M. Kowalska, D. Lunney, S. Naimi, D. Neidherr, H. Schatz, S. Schwarz, L. Schweikhard, Physical Review C 80 (2009) 035805.
[30] F. Herfurth, G. Audi, D. Beck, K. Blaum, G. Bollen, P. Delahaye, M. Dworschak, S. George, C. Guénaut, A. Kellerbauer, D. Lunney, M. Mukherjee, S. Rahaman, S. Schwarz, L. Schweikhard, C. Weber, C. Yazidjian, European Physical Journal A 47 (2011) 1–9.
[31] F. Käppeler, H. Beer, K. Wisshak, Reports on Progress in Physics 52 (1989) 945.
[32] F. Käppeler, R. Gallino, S. Bisterzo, W. Aoki, Reviews on Modern Physics 83 (2011) 157–193.
[33] C. Fröhlich, G. Martinez-Pinedo, M. Liebendörfer, F.-K. Thielemann, E. Bravo, W.R. Hix, K. Langanke, N.T. Zinner, Physical Review Letters 96 (2006) 142502.
[34] C. Weber, V.-V. Elomaa, R. Ferrer, C. Fröhlich, D. Ackermann, J. Äystö, G. Audi, L. Batist, K. Blaum, M. Block, A. Chaudhuri, M. Dworschak, S. Eliseev, T. Eronen, U. Hager, J. Hakala, F. Herfurth, F.P. Heßberger, S. Hofmann, A. Jokinen, A. Kankainen, H.-J. Kluge, K. Langanke, A. Martín, G. Martínez-Pinedo, M. Mazzocco, I.D. Moore, J.B. Neumayr, Y.N. Novikov, H. Penttilä, W.R. Plaß, A.V. Popov, S. Rahaman, T. Rauscher, C. Rauth, J. Rissanen, D. Rodríguez, A. Saastamoinen, C. Scheidenberger, L. Schweikhard, D.M. Seliverstov, T. Sonoda, F.-K. Thielemann, P.G. Thirolf, G.K. Vorobjev, Physical Review C 78 (2008) 054310.
[35] G. Gräff, H. Kalinowsky, J. Traut, Zeitschrift für Physik A Hadrons and Nuclei 297 (1980) 35–39.
[36] G. Bollen, P. Dabkiewicz, P. Egelhof, T. Hilberath, H. Kalinowsky, F. Kern, H. Schnatz, L. Schweikhard, H. Stolzenberg, R. Moore, H.-J. Kluge, G. Temmer, G. Ulm, Hyperfine Interactions 38 (1987) 793–802.
[37] H. Stolzenberg, S. Becker, G. Bollen, F. Kern, H.-J. Kluge, T. Otto, G. Savard, L. Schweikhard, G. Audi, R.B. Moore, Physical Review Letters 65 (1990) 3104–3107.
[38] M. Mukherjee, D. Beck, K. Blaum, G. Bollen, J. Dilling, S. George, F. Herfurth, A. Herlert, A. Kellerbauer, H.J. Kluge, S. Schwarz, L. Schweikhard, C. Yazidjian, European Physical Journal A 35 (2008) 1–29.
[39] H.-J. Kluge, Penning trap mass spectrometry of radionuclides, in this issue.
[40] E. Kugler, Hyperfine Interactions 129 (2000) 23–42.
[41] W. Tretner, Vacuum 10 (1960) 31–34.
[42] H. Wollnik, M. Przewloka, International Journal of Mass Spectrometry and Ion Processes 96 (1990) 267–274.
[43] H. Wollnik, History of mass measurements using time-of-flight techniques, in this issue.
[44] C. Scheidenberger, F. Attallah, A. Casares, U. Czok, A. Dodonov, S.A. Eliseev, H. Geissel, M. Hausmann, A. Kholomeev, V. Kozlovski, Y.A. Litvinov, M. Maier, G. Münzenberg, N. Nankov, Y.N. Novikov, T. Radon, J. Stadlmann, H. Weick, M. Weidenmuller, H. Wollnik, Z. Zhou, Hyperfine Interactions 132 (2001) 531–534.
[45] H. Wollnik, A. Casares, Hyperfine Interactions 132 (2001) 439–442.
[46] Y. Ishida, M. Wada, Y. Matsuo, I. Tanihata, A. Casares, H. Wollnik, Nuclear Instruments and Methods in Physics Research B 219/220 (2004) 468–472.
[47] W.R. Plaß, T. Dickel, U. Czok, H. Geissel, M. Petrick, K. Reinheimer, C. Scheidenberger, M.I. Yavor, Nuclear Instruments and Methods in Physics Research B 266 (2008) 4560–4564.
[48] Y. Ishida, M. Wada, H. Wollnik, Nuclear Instruments and Methods in Physics Research B 241 (2005) 983–985.
[49] A. Verentchikov, M. Yavor, Y. Hasin, M. Gavrik, Technical Physics 50 (2005) 73–81.
[50] A. Verentchikov, M. Yavor, Y. Hasin, M. Gavrik, Technical Physics 50 (2005) 82–86.
[51] W.R. Plaß, T. Dickel, M. Petrick, D. Boutin, Z. Di, T. Fleckenstein, H. Geissel, C. Jesch, C. Scheidenberger, Z. Wang, European Physical Journal Special Topics 150 (2007) 367–368.
[52] A. Piechaczek, V. Shchepunov, H. Carter, J. Batchelder, E. Zganjar, S. Liddick, H. Wollnik, Y. Hu, B. Griffith, Nuclear Instruments and Methods in Physics Research B 266 (2008) 4510–4514.
[53] P. Schury, K. Okada, S. Shchepunov, T. Sonoda, A. Takamine, M. Wada, H. Wollnik, Y. Yamazaki, European Physical Journal A 42 (2009) 343–349.
[54] R.N. Wolf, D. Beck, K. Blaum, Ch. Böhm, Ch. Borgmann, M. Breitenfeldt, F. Herfurth, A. Herlert, M. Kowalska, S. Kreim, D. Lunney, S. Naimi, D. Neidherr, M. Rosenbusch, L. Schweikhard, J. Stanja, F. Wienholtz, K. Zuber, Nuclear Instruments and Methods in Physics Research A 686 (2012) 82–90.
[55] W.R. Plaß et. al., in this issue.
[56] D. Zajfman, O. Heber, L. Vejby-Christensen, I. Ben-Itzhak, M. Rappaport, R. Fishman, M. Dahan, Physical Review A 55 (1997) R1577–R1580.
[57] W.H. Benner, Analytical Chemistry 69 (1997) 4162–4168.
[58] P. Reinhed, A. Orban, S. Rosen, R.D. Thomas, I. Kashperka, H.A.B. Johansson, D. Misra, A. Fardi, L. Brannholm, M. Bjorkhage, H. Cederquist, H.T. Schmidt, Nuclear Instruments and Methods in Physics Research A 621 (2010) 83–90.
[59] M. Lange, M. Froese, S. Menk, J. Varju, R. Bastert, K. Blaum, J.R.C. López-Urrutia, F. Fellenberger, M. Grieser, R. von Hahn, O. Heber, K.-U. Kühnel, F. Laux, D.A. Orlov, M.L. Rappaport, R. Repnow, C.D. Schröter, D. Schwalm, A. Shornikov, T. Sieber, Y. Toker, J. Ullrich, A. Wolf, D. Zajfman, Review of Scientific Instruments 81 (2010) 055105.
[60] J.B. Greenwood, O. Kelly, C.R. Calvert, M.J. Duffy, R.B. King, L. Belshaw, L. Graham, J.D. Alexander, I.D. Williams, W.A. Bryan, I.C.E. Turcu, C.M. Cacho, E. Springate, Review of Scientific Instruments 82 (2011) 043103.
[61] M.W. Froese, M. Lange, S. Menk, M. Grieser, O. Heber, F. Laux, R. Repnow, T. Sieber, Y. Toker, R. von Hahn, A. Wolf, K. Blaum, New Journal of Physics 14 (2012) 073010.
[62] G. Bollen, H.-J. Kluge, M. König, T. Otto, G. Savard, H. Stolzenberg, R.B. Moore, G. Rouleau, G. Audi, Collaboration I Physical Review C 46 (1992) R2140–R2143.
[63] D. Beck, F. Ames, M. Beck, G. Bollen, B. Delauré, P. Schuurmans, S. Schwarz, P. Schmidt, N. Severijns, O. Forstner, Hyperfine Interactions 132 (2001) 469–474.
[64] S. Sturm, K. Blaum, M. Breitenfeldt, P. Delahaye, A. Herlert, L. Schweikhard, F. Wenander, Non-Neutral Plasma Physics VII: Workshop on Non-Neutral Plasmas 2008, vol. 1114, 2009, pp. 185–190.
[65] A. Herlert, Ch. Borgmann, D. Fink, C. Holm Christensen, M. Kowalska, S. Naimi, Hyperfine Interactions 199 (2011) 211–220.
[66] A. Gustafsson, A. Herlert, F. Wenander, Nuclear Instruments and Methods in Physics Research A 626 (2011) 8–15.
[67] Ch. Borgmann, Ph.D. thesis, Ruprecht-Karls-Universität Heidelberg, 2012.
[68] F. Herfurth, J. Dilling, A. Kellerbauer, G. Bollen, S. Henry, H. Kluge, E. Lamour, D. Lunney, R. Moore, C. Scheidenberger, S. Schwarz, G. Sikler, J. Szerypo, Nuclear Instruments and Methods in Physics Research A 469 (2001) 254–275.
[69] N.E. Bradbury, R.A. Nielsen, Physical Review 49 (1936) 388–393.
[70] G. Savard, S. Becker, G. Bollen, H.-J. Kluge, R. Moore, T. Otto, L. Schweikhard, H. Stolzenberg, U. Wiess, Physics Letters A 158 (1991) 247–252.
[71] D. Fink, J. Barea, D. Beck, K. Blaum, Ch. Böhm, Ch. Borgmann, M. Breitenfeldt, F. Herfurth, A. Herlert, J. Kotila, M. Kowalska, S. Kreim, D. Lunney, S. Naimi, M. Rosenbusch, S. Schwarz, L. Schweikhard, F. Šimkovic, J. Stanja, K. Zuber, Physical Review Letters 108 (2012) 062502.
[72] M. Kowalska, S. Naimi, J. Agramunt, A. Algora, D. Beck, B. Blank, K. Blaum, Ch. Boehm, Ch. Borgmann, M. Breitenfeldt, L.M. Fraile, S. George, F. Herfurth, A. Herlert, S. Kreim, D. Lunney, E. Minaya-Ramirez, D. Neidherr, M. Rosenbusch, B. Rubio, L. Schweikhard, J. Stanja, K. Zuber, Nuclear Instruments and Methods in Physics Research A 689 (2012) 102–107.
[73] R.N. Wolf, M. Eritt, G. Marx, L. Schweikhard, Hyperfine Interactions 199 (2011) 115–122.
[74] R.N. Wolf, G. Marx, M. Rosenbusch, L. Schweikhard, International Journal of Mass Spectrometry 313 (2012) 8–14.
[75] O.K. Yoon, I.A. Zuleta, M.D. Robbins, G.K. Barbula, R.N. Zare, Journal of the American Society for Mass Spectrometry 18 (2007) 1901–1908.
[76] W.C. Wiley, I.H. McLaren, Review of Scientific Instruments 26 (1955) 1150–1157.
[77] P.V. Duppen, Nuclear Instruments and Methods in Physics Research B 204 (2003) 9–16.
[78] Y. Blumenfeld, T. Nilsson, P.V. Duppen, Physica Scripta T152 (2013) 014023.
[79] V.N. Fedosseev, L.-E. Berg, D.V. Fedorov, D. Fink, O.J. Launila, R. Losito, B.A. Marsh, R.E. Rossel, S. Rothe, M.D. Seliverstov, A.M. Sjodin, K.D.A. Wendt, Review of Scientific Instruments 83 (2012) 02A903.
[80] V. Fedosseev, D. Fedorov, R. Horn, G. Huber, U. Köster, J. Lassen, V. Mishin, M. Seliverstov, L. Weissman, K. Wendt, Nuclear Instruments and Methods in Physics Research B 204 (2003) 353–358.
[81] B. March et al., Proceedings of the 16th International Conference on Electromagnetic Isotope Separators and Techniques Related to their Applications, Nuclear Instruments and Methods in Physics Research B, submitted for publication.
[82] G. Audi, F. Kondev, M. Wang, B. Pfeiffer, X. Sun, J. Blachot, M. MacCormick, Chinese Physics C 36 (2012) 1157.
[83] A. Kellerbauer, K. Blaum, G. Bollen, F. Herfurth, H.-J. Kluge, M. Kuckein, E. Sauvan, C. Scheidenberger, L. Schweikhard, European Physical Journal D 22 (2003) 53–64.
[84] M. Wang, G. Audi, A. Wapstra, F. Kondev, M. MacCormick, X. Xu, B. Pfeiffer, Chinese Physics C 36 (2012) 1603–2014.
[85] R.N. Wolf, D. Beck, K. Blaum, Ch. Böhm, Ch. Borgmann, M. Breitenfeldt, N. Chamel, S. Goriely, F. Herfurth, M. Kowalska, S. Kreim, D. Lunney, V. Manea, E. Minaya Ramirez, S. Naimi, D. Neidherr, M. Rosenbusch, L. Schweikhard, J. Stanja, F. Wienholtz, K. Zuber, Physical Review Letters 110 (2013) 041101.
[86] M. Madurga, R. Surman, I.N. Borzov, R. Grzywacz, K.P. Rykaczewski, C.J. Gross, D. Miller, D.W. Stracener, J.C. Batchelder, N.T. Brewer, L. Cartegni, J.H. Hamilton, J.K. Hwang, S.H. Liu, S.V. Ilyushkin, C. Jost, M. Karny, A. Korgul, W. Królas, A. Kuźniak, C. Mazzocchi, A.J.I.I. Mendez, K. Miernik, S.W. Padgett, S.V. Paulauskas, A.V. Ramayya, J.A. Winger, M. Wolińska-Cichocka, E.F. Zganjar, Physical Review Letters 109 (2012) 112501.
[87] P. Bolotskikh, D. Grinfeld, A. Makarov, M. Monastyrskiy, Nuclear Instruments and Methods in Physics Research A 645 (2011) 146–152.
[88] M. Rosenbusch, S. Kemnitz, R. Schneider, L. Schweikhard, R. Tschiersch, R.N. Wolf, AIP Conference Proceedings 1521 (2013) 53–62.
[89] M. Rosenbusch, in preparation.
[90] G. Bollen, Nuclear Physics A 693 (2001) 3–18.
[91] S. Eliseev, C. Roux, K. Blaum, M. Block, C. Droese, F. Herfurth, M. Kretzschmar, M.I. Krivoruchenko, E. Minaya Ramirez, Y.N. Novikov, L. Schweikhard, V.M. Shabaev, F. Šimkovic, I.I. Tupitsyn, K. Zuber, N.A. Zubova, Physical Review Letters 107 (2011) 152501.
[92] S. Eliseev, K. Blaum, M. Block, C. Droese, M. Goncharov, E. Minaya Ramirez, D. Nesterenko, Yu.N. Novikov, L. Schweikhard, Physical Review Letters 110 (2013) 082501.
[93] M. Rosenbusch, K. Blaum, C. Borgmann, S. Kreim, M. Kretzschmar, D. Lunney, L. Schweikhard, F. Wienholtz, R.N. Wolf, Int. J. Mass Spectrom. 325–327 (2012) 51–57.
[94] F. Wienholtz, in preparation.
[95] F. Wienholtz, D. Beck, K. Blaum, Ch. Borgmann, M. Breitenfeldt, R.B. Cakirli, S. George, F. Herfurth, J.D. Holt, M. Kowalska, S. Kreim, D. Lunney, V. Manea, J. Menéndez, D. Neidherr, M. Rosenbusch, L. Schweikhard, A. Schwenk, J. Simonis, J. Stanja, R.N. Wolf, K. Zuber, accepted for publication.

Please cite this article in press as: R.N. Wolf, et al., Int. J. Mass Spectrom. (2013), http://dx.doi.org/10.1016/j.ijms.2013.03.020